25

Residual Stresses and Cracking in Dental Restorations due to Resin Contraction Considering In-Depth Young's Modulus Variation

Estevam Barbosa de Las Casas, João Batista Novaes Jr.,
Elissa Talma, Willian Henrique Vasconcelos,
Tulimar P. Machado Cornacchia, Iracema Maria Utsch Braga,
Carlos Alberto Cimini Jr. and Rodrigo Guerra Peixoto
Universidade Federal de Minas Gerais
Universidade de Campinas
Brazil

1. Introduction

Composite resins have been increasingly used as restorative material, both in anterior and posterior teeth, where they replace metal restorations. Its aesthetic characteristics, coupled with improved physical properties have made their use extend from just anterior teeth to also include posterior teeth. The use of such material in oral regions subjected to higher loading makes it important to account for the effect of residual stresses arising during polymerization, induced by resin contraction (Ausiello, Apicilla and Davidson 2002). Different reports can be found in the literature focused in this aspect and using different approaches, such as X-ray micro-computed tomography (Sun, Eidelman and Gibson 2009), 3D evaluation of the marginal adaptation (Kakaboura et al 2007) and 3 D deformation analysis from MCT images (Chiang et al 2010). These authors agree in the critical role played by resin contraction in restoration success. The Finite Element Method can therefore be a useful tool to investigate the cracking of interfaces, stress concentrations in the internal angles and effects of variations in the mechanical properties in the overall behavior of the resin-based dental restorations.

Some composite resins for dentistry use are the result of the interaction of an organic matrix, a coupling agent and an inorganic material, since it was first devised by Bowen et al. (1983). In the last decades, industry has altered significantly the inorganic part of this composition. As a result, composite hybrid resins, with the inclusion of nanoparticles have not only improved strength and abrasion resistance but also presented greater polishing characteristics. Nevertheless, their physicochemical properties are still dependent of the polymerization of the resin matrix, induced by light penetration with 400 to 500 nm wave lengths, the peak absorption of camphorquinone (Braga et al., 2005).

The beginning of the polymerization process of the resinous matrix happens when it is irradiated with an external source, and stops when the maximum conversion of the monomers is reached, which varies with time of exposure to light, quality of the polymerizing agent and depth of light penetration (Jandt et al., 2000; Felix et al., 2006; Jong et al., 2007; Ceballos et al., 2009; Ferracane, 2005). The degree of conversion of the resin matrix can then be associated directly to the physical properties of the restoration, as well as its strength under dental loading (Peutzfeldt et al., 2000; Sakaguchiet al., 1991).

When a composed resin is applied directly to dental tissues, after the hybridization by the adhesive agent of the cavity walls, the requirement is to rigidly connect enamel and dentine to the restoring material, in the attempt to generate a solid and continuous body as a mechanically ideal restoration. The ideal restoration would be totally impermeable to the infiltration of fluids and resistant to the opening of gaps in the tooth-restoration interface.

The use of the composed resin as restorative material implies in the polymerization of the resinous matrix and in its fixation to the cavity walls. However, during the polymerization the resinous matrix suffers contraction, which can surpass the adhesive rupture resistance, leading to imperfections in the restoration as marginal gaps, cracking, hypersensitivity and infiltration. The reduction of the generated residual stresses can be obtained in different ways during polymerization: (i) when a controlled fluid flow is allowed during the process (Braga et al.,2005); (ii) by the use of devices with the *soft-start* technique (Yoshikawa et al., 2001); (iii) reducing the associated factor C in the layers deposition (Ceballos et al., 2009; Petrovic et al., 2010); (iv) through the application of resinous material with low modulus of elasticity that can deform without producing high residual stresses (Dietschi et al., 2002); and (v) using a method of improving marginal adaptation by eliminating stress concentration points during resin photo-polymerization (Petrovic et al., 2010).

After polymerization, the composite resin exposition to the humid oral environment leads to water penetration to the inner regions of the restored cavity, causing volumetric hygroscopic expansion. Due to the penetration of water inside the hydrophilic organic matrix, a gradual expansion occurs, until a balanced value is eventually reached.

The aim of this study is to quantify the effect of the use of two different irradiation sources (halogen and second-generation LED) on the elastic modulus and the degree cure during the polymerization process of a nanofilled composite restorative material. The effect of the variation of the elastic modulus on the polymerization residual stresses is then accessed by means of3-D finite element simulations, in order to understand the mechanical response of a cylindrical Class I restoration under polymerization contraction.

2. Material and methods

2.1 Evaluation of composite resin mechanical properties

A composite resin (Filtek Z250, 3M Co., St Paul., MN, USA) and two different irradiation sources, XL3000 (halogen - 3M) and Elipar Freeligth 2 (LED - 3M ESPE), were used to evaluate, *in vitro*, the degree of conversion and the Young's modulus (also modulus of elasticity or elastic modulus) distribution along sample height. This last parameter was then used to examine, through a computer simulation, the effect of through-height stiffness variation in expected polymerization residual stresses.

2.1.1 Evaluation of the Degree of Conversion

To measure the Degree of Conversion (DC), test samples were prepared in standardized plastic molds with diameter of 4 mm and height of 2 mm and 4 mm. Four groups of samples were prepared, each one with three samples (n=3). Three measurements were performed for each sample. The groups were classified as: Group 1 (G1) – XL 3000, 2 mm height; Group 2 (G2) – Elipar, 2 mm height; Group 3 (G3)– XL3000, 4 mm height; Group 4 (G4) – Elipar, 4 mm height. The moulds were filled to the top in one step, and irradiated during a period of 40 seconds. After that, they were stored in a dark environment. The Degree of Conversion (DC) was measured at the base of the samples. Raman spectra were obtained on a JobinYvon/Horiba LABRAM-HR 800 spectrograph equipped with a He-Ne laser (632.8nm). The power in each sample was around 7mW. The Raman signal was collected by an Olympus BHX microscope provided with objectives (10x, 50x and 100x). The detector used was a N_2 liquid cooled CCD (Charge-Couple Device) of the Spectrum One, back illuminated. Depending on the sample background fluorescence, the acquisition time ranged from 10 to 30 seconds. To reduce signal/noise ratio, spectra were acquired 5 times after a 5 minutes photobleaching. Collected Raman spectra were analyzed and optimized with Labspec 1.1 and PeakFit v4. Spectra collected were averaged. The background was corrected and if necessary, normalized and peak deconvoluted.

The samples were excited by laser in the region between 2000 to 1000 cm^{-1} after five 60 second accumulations in order to evaluate the conversion proportion of the vinylic function in aliphatic function, comparing the residual non-polymerized methacrylate band C=C (1640cm^{-1}) to the aromatic 1610cm^{-1} C=C stretching band used as reference. The DC value was defined as given in Eq. (1),

$$DC(\%) - 100x\,[1 - Rp/\,Rnp] \tag{1}$$

where Rp and Rnp are the signals for the polymerized resin and non-polymerized resin. The degree of conversion was determined at three locations and the mean value calculated for each of the three specimens. From these three averages a new mean value was calculated.

2.1.2 Young's modulus measurement

Three specimens were prepared for each condition in order to measure the modulus of elasticity (Young's modulus) and were stored dry at room temperature for at least 24 hours before testing. All these specimens were prepared with 4 mm height, and the radiation source was kept at a distance between 1 and 2 mm. Therefore, there were also four groups of specimens for Young's modulus measurement: Group 1 (G1) – XL 3000, light source at 1 mm distance; Group 2 (G2) – XL3000, light source at 2 mm distance; Group 3 (G3)–Elipar, light source at 1 mm distance; Group 4 (G4) – Elipar, light source at 2 mm distance. For each group, three specimens were made (n=3) and, for each specimen, three indentations were done at four different depths (0.5, 1.5, 2.5 and 3.5 mm). The indentations were performed using a micro-durometer Shimadzu, at a speed of 2.6 mN/sand kept for 5 seconds. The values of Young's modulus and hardness were obtained for each depth in order to detect through-depth changes in the mechanical properties.

2.2 Finite element simulation

To simulate the restoration, a cylindrical model with a cavity was created to represent the dentine. On the cavity's inner walls an adhesive layer was applied, followed by the resin addition and then polymerization is performed. Despite being an axisymmetric problem, a three dimensional model was necessary due to software limitations to represent the adhesive material. Previous works in the literature describe numerical analysis of resin expansion, but disregarded the stiffness variation due to the light activation of the resin (Rüttermann et al., 2007; Carvalho Filho, 2005; Ausiello et al., 2002).

To simulate both the dentine and the resin regions, ten-nodded tetrahedral elements were used, with three degrees of freedom at each node. Program Ansys, release 10, was used in the analyses. Figure 1 represents the geometry of the model. A special element with a constitutive model developed for brittle materials was used for the adhesive layer in order to simulate cracking. This material constitutive model has a cutoff that imposes a limit to normal and tangential stresses, after which fracture occurs.

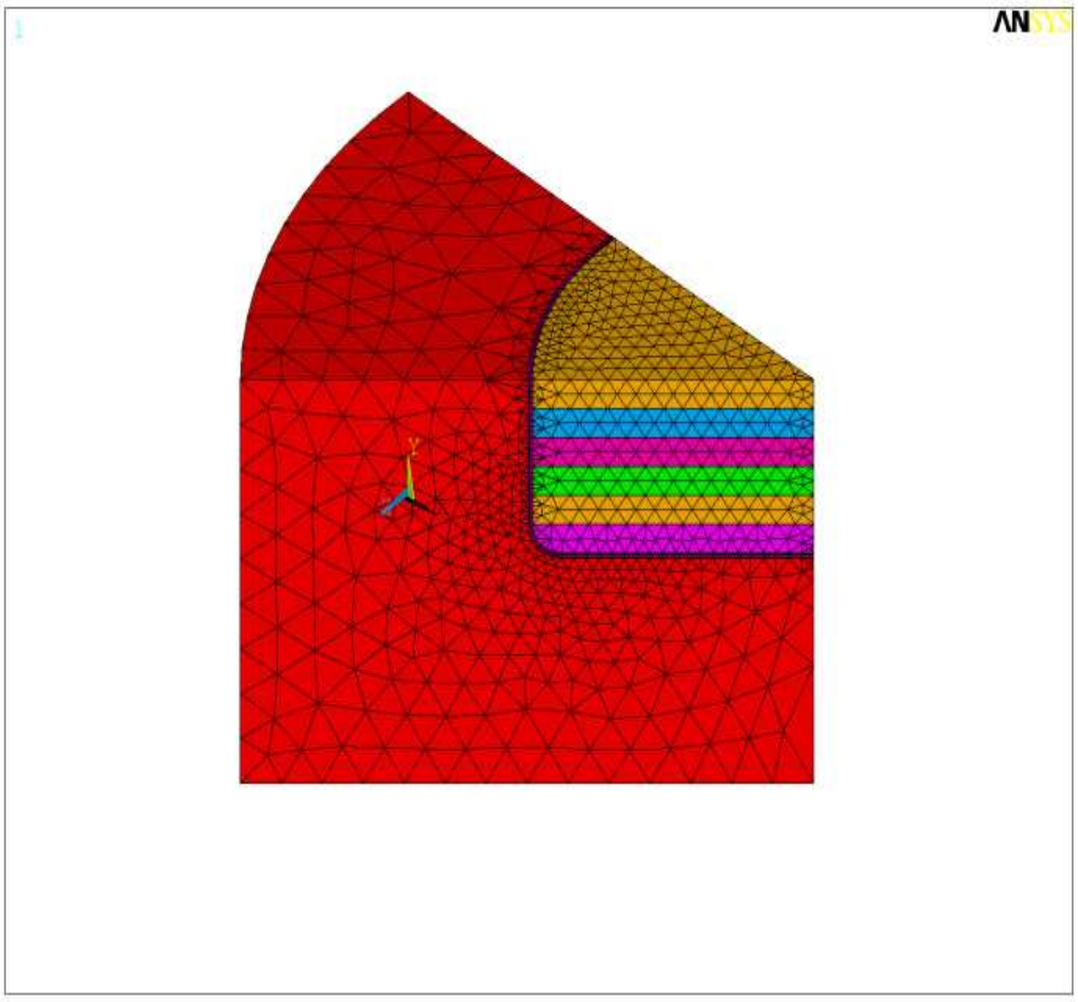

Fig. 1. Geometric model

Boundary conditions were imposed so as to restrict displacements at the base and non-vertical displacements in the faces, consistent with the restoration axisymmetry. Figure 2 shows dentine with the cavity, and Table 1 its material properties according to Ausiello et al. (2002). It is assumed that the dentine is under small displacements, with elastic behavior, and there is no stiffness variation. It is also considered homogeneous and isotropic. The analysis is then linear for this component.

The adhesive is represented by a thin layer with low traction strength. This material model introduces a nonlinear effect to the model, besides demanding a three dimensional geometric model. The traction at the interface was limited to 45 MPa, as indicated in the literature (Ausielo et al, 2002). In the process of solving the equations, the program verifies if this limit is exceeded at each iteration. If so, a crack is generated. Later, if compression at a normal direction to the crack's plane occurs, the crack is closed.

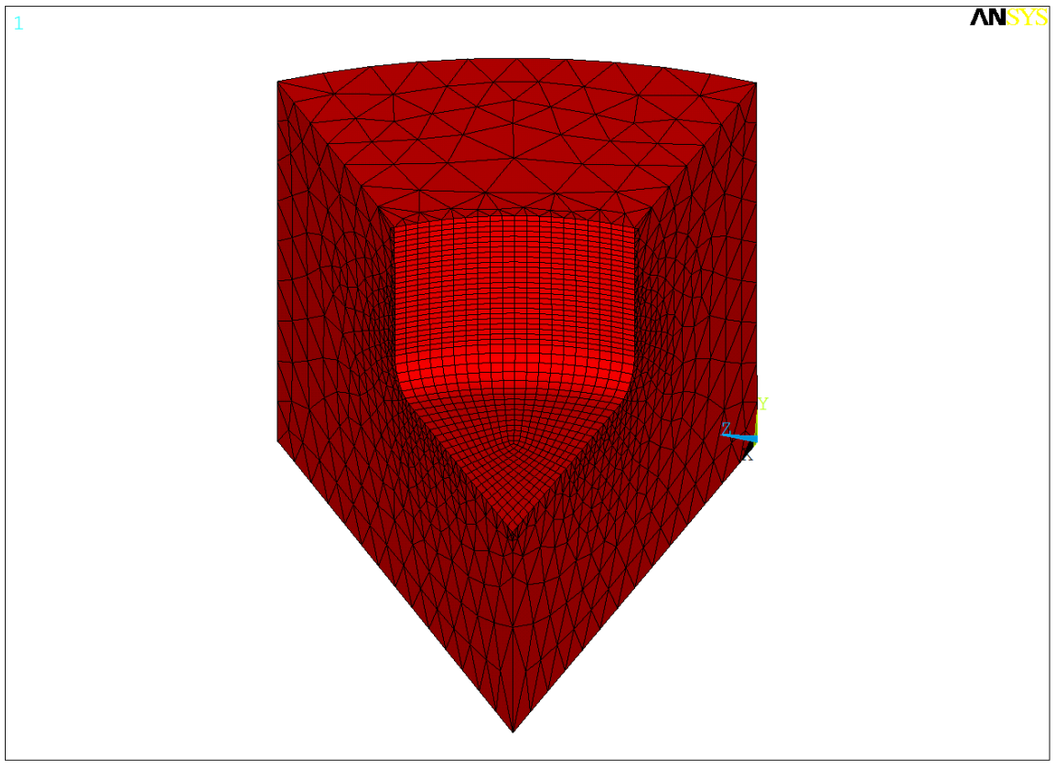

Fig. 2. Discrete model

Material	Young's Modulus	Poisson ratio
Dentine	18000 MPa	0.31
Adhesive	1000 MPa	0.30

Table 1. Material properties for dentine and adhesive (Ausielo et al, 2002)

Figure 3 shows the adhesive layer, and Table 1 presents its material mechanical properties (Ausielo et al, 2002).

The geometry of the resin was divided in six layers, each one with a half millimeter height. To these layers different values for the Young's modulus were assigned, which were measured from the laboratory experiments, as described in item 2.1.2.

In order to impose a volumetric contraction, a thermal expansion coefficient was introduced, and set to 0.01 $^{o}C^{-1}$. Then, a temperature variation was applied to the resin in the model, being negative to contraction and positive to expansion, calculated so as to produce the desired resin contraction.

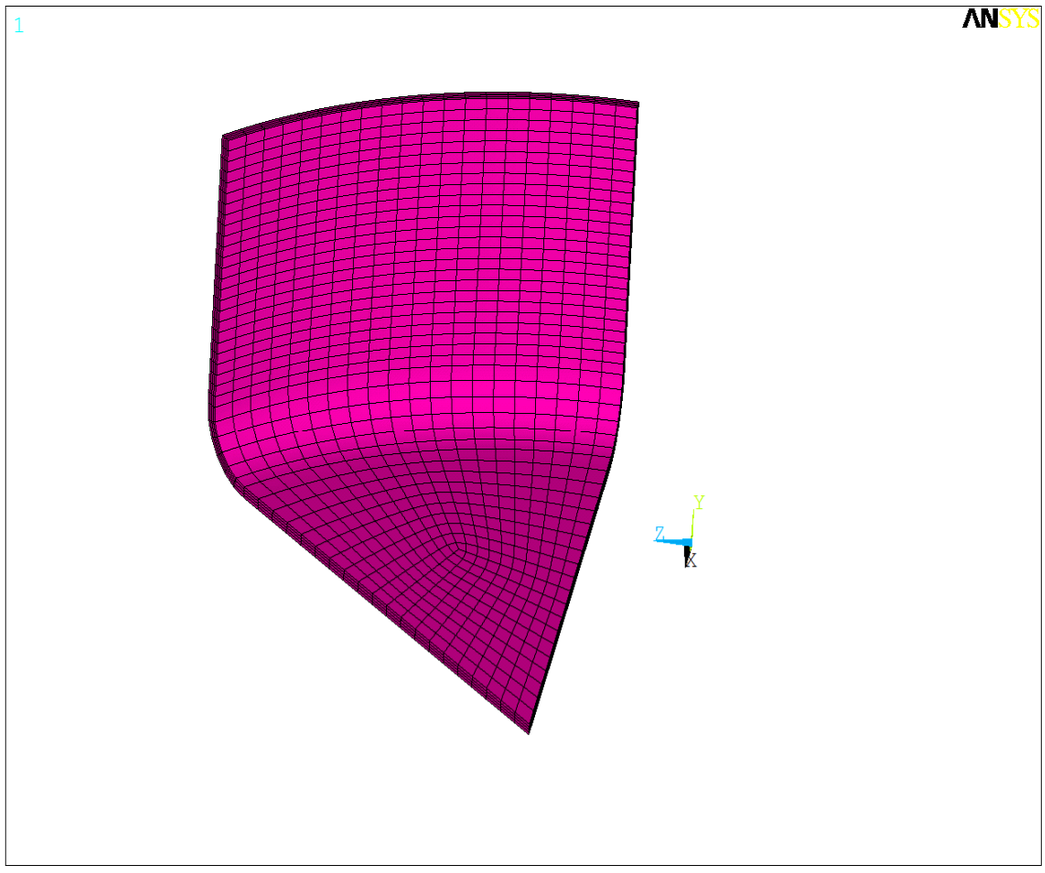

Fig. 3. Interface layer model

Two different clinical situations were studied. First, the cavity complete filling in a single step (here called "*one increment technique*"), consisting in filling the whole cavity with resin and then polymerizing it in one step. Then, the cavity filling in steps (here called "*horizontal incremental technique*") consisting in filling the cavity with resin one layer at a time, polymerizing it and moving to the next, outer layer. A new layer of resin is added, and the process is repeated until the resin reaches the top of the cavity. This way, the layers will be thin, causing less stiffness variation, as indicated by the experimental results. For this study, the cavity was considered filled with three increments of equal thickness.

In the first method (one increment technique) the Young's modulus variation is significant, and its value will be smaller on the top of the restoration. The polymerization is simulated

using the *Birth and Death* resource available in the software, which reduces the "dead" element's stiffness to a very low value, practically eliminating the contribution of that region's stiffness from the analysis. This resource allows the user to activate only part of the domain in one step, and then consider previously "dead" regions for further load steps.

To simulate the horizontal incremental technique, three layers were created. The two lowest were initially "killed" and a temperature variation applied at the top layer. The numerical system was solved. Then, the middle layer was "born" or activated, the temperature variation was applied, and the new system was solved. The same process was followed by the third layer.

This technique of simulation was similar to the one increment technique, but now the layers were polymerized from the bottom to the top, with the layer activation sequence following a downward sequence. An incremental iterative Newton-Raphson algorithm with a force based convergence criteria was used. The stopping criterion is given in Eq. (2), with $\beta = 0.001$ (F_{int} is the internal force and F_{ext} is the external force):

$$\left\| F_{int} - F_{ext} \right\| < \beta \cdot \left\| F_{ext} \right\| \tag{2}$$

3. Results

3.1 Degree of Conversion (DC)

The Raman test results for XL3000 (G1 and G3) and Elipar (G2 and G4) groups are respectively presented in Figures 4 and 5.

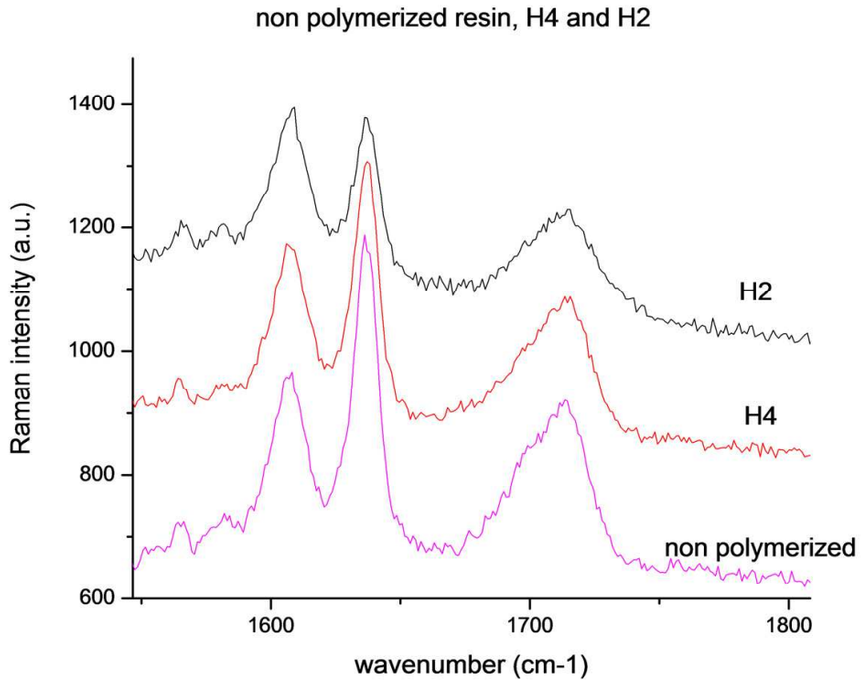

Fig. 4. Raman test results for XL3000 polymerization device and thicknesses of 2 mm (H2-G1) and 4mm (H4-G3)

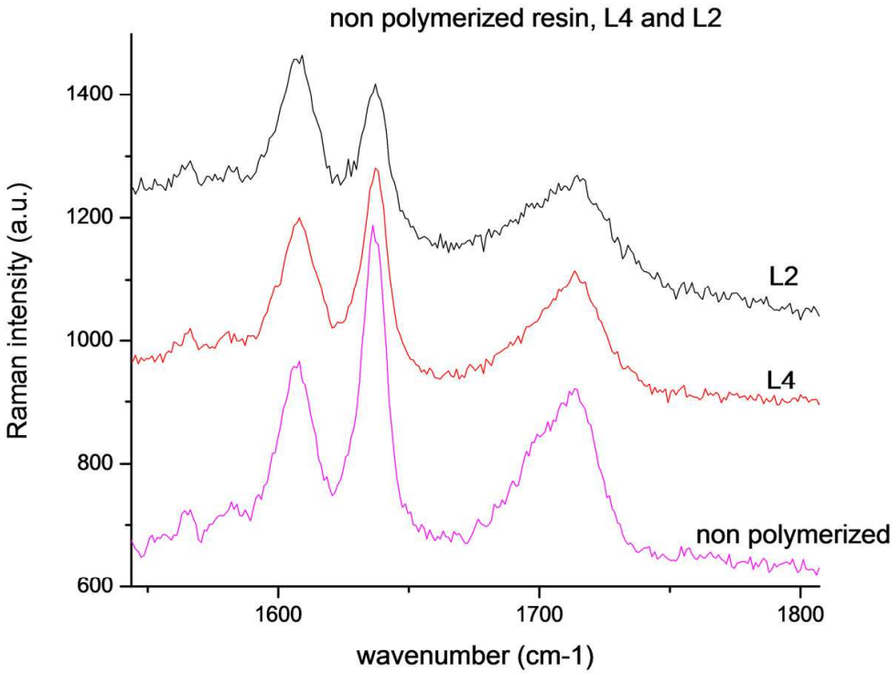

Fig. 5. Raman test results for Elipar polymerization device and thicknesses of 2 mm (L2-G2) and 4mm (L4-G4)

The measured average degrees of conversion values are listed in Table 2 for the four groups.

Sample height	XL3000 - QTH		Elipar Freeligth 2 - LED	
2mm	55 %	±3 %	59%	± 3 %
4mm	26%	± 1 %	32%	± 2 %

Table 2. Degree of conversion (in %) for Z350 resin measured using the Raman technique

The results for DC fit into a normal distribution, and three-way ANOVA model was used to analyze the influence of mode of cure sample height. Comparisons of the QTH (XL3000) and LED (Elipar Freeligth 2) curing methods showed significant influence of initial height in the degree of conversion ($p < 0.05$). For higher initial height, it was observed a sharp reduction in DC values. As for different irradiation techniques, it did not produce significant difference between the groups with the same initial height (2 or 4mm).

3.2 Young's modulus

The Young's modulus (E) showed a decrease for points located farther away from the light sources, as it is shown in Table 3, for both curing methods, regardless of the distance between the sample and the light source.

Group-depth	E (GPa)		W	p
	Average	Std Dev		
G1-0.5 mm	20.094	1.4360	0.678	0.0089
G1-1.5 mm	19.375	0.6461	0.9526	0.6901
G1-2.5 mm	17.720	0.8739	0.9351	0.9351
G1-3.5 mm	12.288	1.7453	0.9194	0.4180
G2-0.5 mm	19.004	1.4362	0.8287	0.0497
G2-1.5 mm	18.071	1.1987	0.838	0.0649
G2-2.5 mm	15.947	0.7665	0.9426	0.5816
G2-3.5 mm	10.755	0.6570	0.9247	0.4457
G3-0.5 mm	19.288	2.0709	0.9658	0.8331
G3-1.5 mm	18.221	1.4476	0.9018	0.3252
G3-2.5 mm	17.146	1.3244	0.9489	0.6501
G3-3.5 mm	15.226	1.2777	0.8505	0.0858
G4-0.5 mm	19.876	1.5748	0.7793	0.0157
G4-1.5 mm	19.056	1.5425	0.9095	0.3659
G4-2.5 mm	18.147	1.2606	0.9711	0.8905
G4-3.5 mm	16.016	1.3564	0.9736	0.9132

Table 3. Young's modulus (in GPa) variations with depth for different curing devices

Comparisons (Dunn method)	Differences	z calculed	z critical	p
G1-0.5mm x G1-1.5mm	2.3333	0.4698	2.638	ns
G1-0.5mm x G1-2.5mm	13.3333	2.6846	2.638	< 0.05
G1-0.5mm x G1-3.5mm	23.2222	4.6757	2.638	< 0.05
G1-1.5mm x G1-2.5mm	11	2.2148	2.638	ns
G1-1.5mm x G1-3.5mm	20.8889	4.2059	2.638	< 0.05
G1-2.5mm x G1-3.5mm	9.8889	1.9911	2.638	ns

Table 4. Young's modulus (in GPa). Variations with depth for group G1, for different depth values, XL3000at distance of 1 mm

Comparisons (Dunn method)	Differences	z calculed	z critical	p
G2-0.5mm x G2-1.5mm	4.5556	0.9172	2.638	ns
G2-0.5mm x G2-2.5mm	15.4444	3.1097	2.638	< 0.05
G2-0.5mm x G2-3.5mm	24.6667	4.9666	2.638	< 0.05
G2-1.5mm x G2-2.5mm	10.8889	2.1924	2.638	ns
G2-1.5mm x G2-3.5mm	20.1111	4.0493	2.638	< 0.05
G2-2.5mm x G2-3.5mm	9.2222	1.8569	2.638	ns

Table 5. Young's modulus (in GPa). Variations with depth for group G2, for different depth values, XL3000 for distance of 2 mm

After verifying that the results do not follow a normal distribution, Kruskal-Wallis analysis was used to statistically determine the significance of the variation in the obtained data. The test did not indicate significant differences in elastic modulus between the depths of 0.5 and 1.5 mm for the QTH device, not even by increasing the position of the polymerization tip by 1 mm. At each 2 mm in depth a statistically significant variation was observed for the elastic modulus.

Comparisons (Dunn method)	Differences	z calculed	z critical	p
G3-0.5mm x G3-1.5mm	3.7222	0.7495	2.638	ns
G3-0.5mm x G3-2.5mm	10.5556	2.1253	2.638	ns
G3-0.5mm x G3-3.5mm	20.1667	4.0605	2.638	< 0.05
G3-1.5mm x G3-2.5mm	6.8333	1.3759	2.638	ns
G3-1.5mm x G3-3.5mm	16.4444	3.311	2.638	< 0.05
G3-2.5mm x G3-3.5mm	9.6111	1.9352	2.638	ns

Table 6. Young's modulus (in GPa). Variations with depth for group G3, for different depth values, Elipar distance of 1mm

Comparisons (Dunn method)	Differences	z calculed	z critical	p
G4-0.5mm x G4-1.5mm	5.3889	1.085	2.638	ns
G4-0.5mm x G4-2.5mm	10	2.0135	2.638	ns
G4-0.5mm x G4-3.5mm	21.5	4.329	2.638	< 0.05
G4-1.5mm x G4 -2.5mm	4.6111	0.9284	2.638	ns
G4-1.5mm x G4-3.5mm	16.1111	3.2439	2.638	< 0.05
G4-2.5mm x G4-3.5mm	11.5	2.3155	2.638	ns

Table 7. Young's modulus (in GPa). Variations with depth for group G4, for different depth values, Elipar distance of 2 mm

For LED polymerization, the results also failed the normality assumption. Kruskal-Wallis analysis did not indicate statistically significant differences in elastic modulus between the depths of 0.5, 1.5 and 2.5 mm for the LED device, not even by increasing the position of the polymerization tip by 1 mm. As for the comparison between 0.5 mm depth and 3.5, $p<0.05$ was obtained, as well as with the distances of 1.5 and 3.5 mm. The LED device showed an improved polymerization performance at 2.5 mm depth, but results showed that at each 2 mm in depth a statistically significant variation has occurred for the elastic modulus.

The variation in the polymerization device`s tip from the sample did not affect the obtained stiffness results, as shown by a comparison between tables 4 and 5 and 6 and 7.

3.3 Numerical results

The mechanical properties for the resin used in the finite element model were the Young's modulus measured at the four different depths presented on Table 8 and the Poisson's ratio equal to 0.3 throughout the resin model. For the finite element simulation it was used the lowest values measured for the Young's modulus (Group 2 – XL3000, light source at 2 mm distance). In this group it was also verified the highest variations on the Young's modulus with respect to the depth (Tables 3 to 7).

Depth (mm)	Young's Modulus (GPa) for the resin	
	Test results for Group 2 (G2) – XL3000, light source at 2 mm distance	Properties used in the Finite Element simulations
0.5	19.004	19.0
1.5	18.071	18.1
2.5	15.947	15.9
3.5	10.755	10.8

Table 8. Young's modulus used in the finite element model (E) for the resin according to depth

The following figures show the first principal stress (σ_1), in MPa, after the polymerization contraction. Figures 6 to 8 show the simulation results for resin contraction in the three-layers horizontal incremental technique. The first principal stresses (σ_1) representing maximum tension are shown, as all the materials have a reduced strength for traction.

Figure 9 depicts the stress values after filling the restoration in a single step (one layer technique). Then, in Fig. 10, the simulation was repeated keeping the Young's modulus for the resin constant, that is, neglecting the variation due to incomplete polymerization. The results are given for both filling techniques.

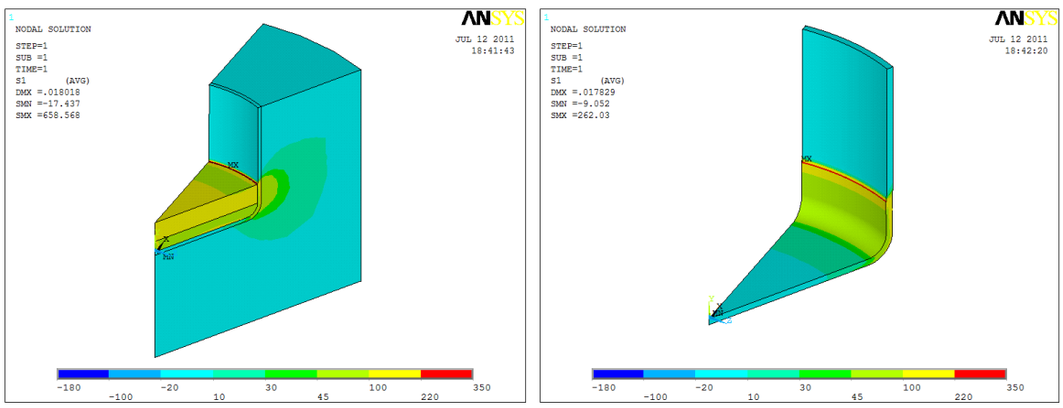

Fig. 6. First principal stresses (σ_1- MPa) for first layer in three-layers horizontal increment technique – restoration on the left and interface on the right

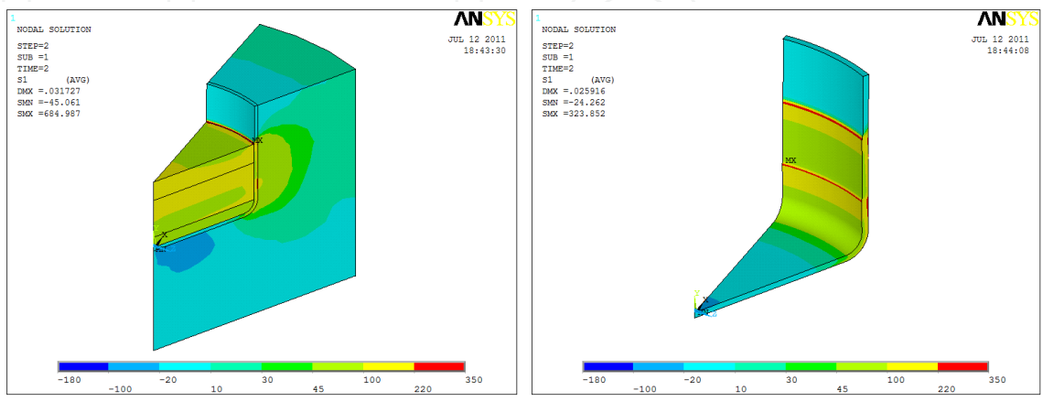

Fig. 7. First principal stresses (σ_1- MPa) for second layer in three-layers horizontal incremental technique – restoration on the left and interface on the right

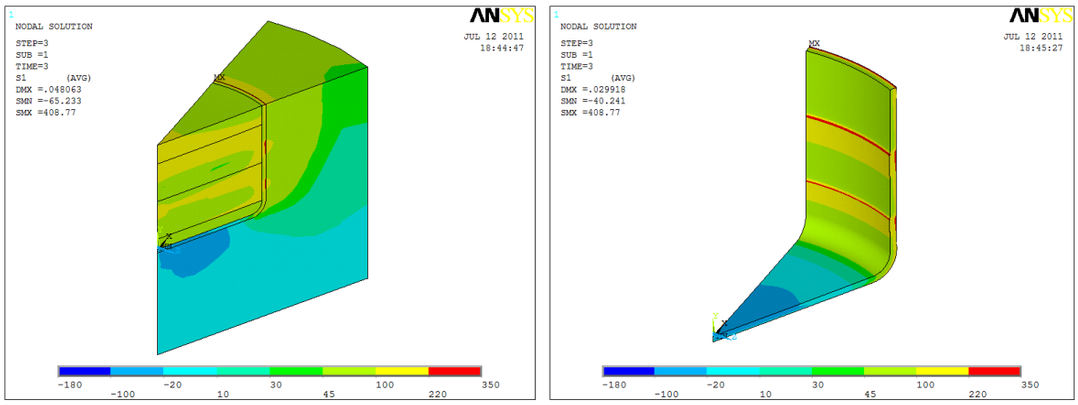

Fig. 8. Final first principal stresses (σ_1- MPa) in three-layers horizontal incremental technique – restoration on the left and interface on the right

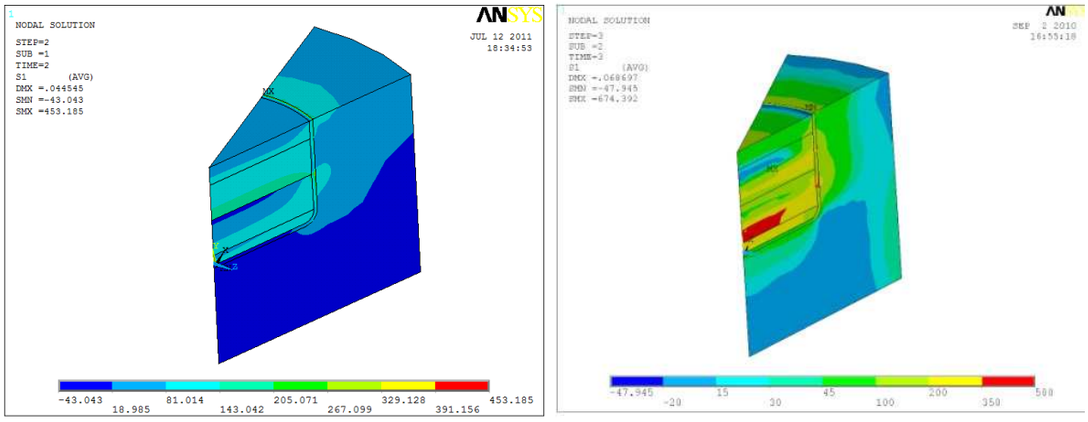

Fig. 9. Final first principal stresses (σ_1- MPa) horizontal incremental technique (2 layers) and one increment (or bulk) filling

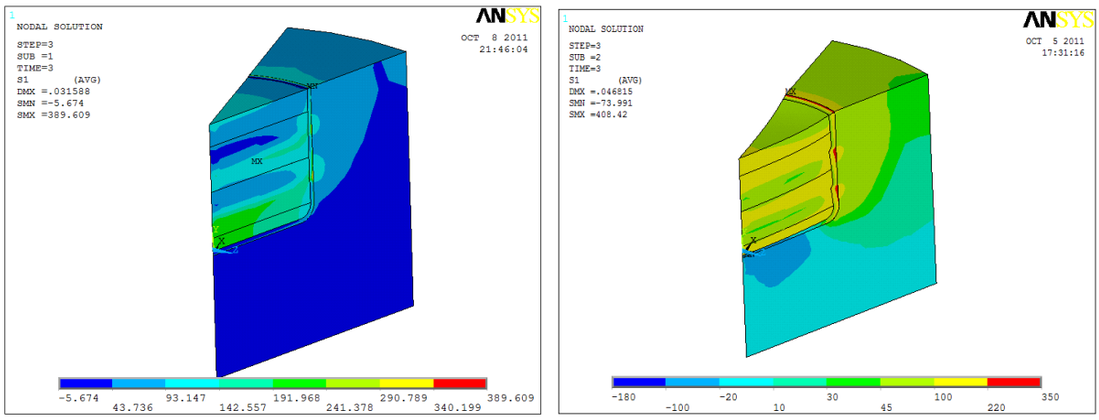

Fig. 10. Final first principal stresses (σ_1- MPa) three and one increment technique with constant E – restoration and dentine

4. Discussion

The study of residual stresses in dental restorations using a finite element simulation tries to reproduce *in silico* a phenomenon frequently observed in dental clinic. By including in the simulation the sequence of cavity filling, the variation in modulus of elasticity resulting from light penetration and the stress relief due to cracking the computational model can represent the process with the inclusion of key aspects of the restoration.

In order to consider the change in properties along the depth of the layers, experimental evaluation of this mechanical property was made, for different light sources and tip positions, as well as for hardness and degree of conversion based on micro-hardness.

Many authors use the degree of conversion associated to harness to verify the effectiveness of the polymerization of composite resins (Kawaguchi et al., 1989; Chung & Greener, 1990). The evaluation of micro-hardness is influenced not only by its degree of conversion, but also by the percentage of filler and presence or absence of oxygen (Peutzfeld, 1997; Yap et al., 2002; Halvorson et al., 2002). As the composite's viscous deformation is a time-dependent event, slower curing rates may provide extended periods where the material is able to yield to contraction forces before acquiring higher elastic modulus (Feilzer et al., 1993). In fact, reducing polymerization rates in composites has been shown to lower stress levels significantly (Bouschlicher & Rueggeberg, 2000; Lim et al., 2002).

There is a direct relationship between the degree of conversion of a resin and its modulus of elasticity. The maximum polymerization of a given resin implies in higher modulus of elasticity and higher contractive stresses in the tooth-resin restoration interface (Davdison-Kaban, 1997). As a consequence, higher mechanical properties for the composite resin results in a corresponding higher value for residual stresses at the adhesive interface (Braem et al., 1987; Silikas et al., 2000).

The degree of conversion was obtained by the Raman method. As for the Young's modulus associated to micro-hardness, the measurements were performed changing the distance from the resin to the tip of the device from 1 to 2 mm. Results showed DC results ranging from 55 and 60% for 2 mm depth, unchanged regardless of the polymerization technique or distance to the tip. For 4 mm depth, DC felt to between 26 and 32% for the two devices, showing a reduction with depth, which can lead to deterioration in its mechanical properties and a reduction in polymerization contraction (Ceballos et al., 2009).

The measurement of the modulus of elasticity showed, for all tested groups, a statistically relevant reduction at each 2 mm depth increase, regardless of the polymerization technology used.

The results obtained for Young's modulus presented a statistically significant reduction for each 2 mm variation in depth, regardless of the curing method. These results reinforce the idea of avoiding to apply layers thicker than 2 mm, which will assure a minimum of non-homogeneity in the material's stiffness, for any restoration volume or configuration factor (Chiang et al., 2010).

According to Dewaele et al. (2009), who investigated different polymerization protocols, the reduction in contraction is directly related to the reduction in the degree of cure. Cho et al. (2011), in an analysis of the particles movement in resin restorations, observed that it

depends on the degree of conversion and the contraction value, and that a mathematical equation can be derived for the particles' displacements, especially for those below a 3.5 mm depth.

The computer simulations show a clear stress concentration between the cavity walls and the restoration material, especially in the regions with more abrupt geometry changes corresponding to restoration internal angles, as well as interface rupture at different points of the wall. Stresses are higher at the interface due to the change in stiffness at that point.. These results agree with the conclusions of Chiang et al. (2010), which also verified gap formation in cylindrical restorations with and without the use of an adhesive layer, both numerically and experimentally, through the use of micro-CT images. Their results pointed to higher stresses for adhesives with smaller modulus of elasticity, sometimes higher than the adhesive limit strength.

Most other regions of the restoration stay under stresses lower than 200 MPa. Stress concentration patterns, that is, final stresses after the polymerization process, are dependent of the curing technique. Stress levels indicate that, without subsequent relief, restoration can be easily damaged by additional loading such as temperature variation or biting. During the polymerization process, as the sequence in Figures 6, 7 and 8 shows, stresses redistribute and vary in the different parts of the restoration, reaching intermediate values that can lead to fracture in the interface and damage at the resin. The limit in stresses at the cement provide a buffer for dentine, as very high stresses are not transmitted through the interface layer, that cracks and avoid compromising the tissue.

As for a comparison between the three polymerization techniques, one, two and three increments, it is evident that higher stresses occur for the last option. Figures 8, 9 and 10 show higher peak stresses at dentine and resin for less incremental filling techniques (two and one layer, respectively).

In Figure 9 different filling techniques are explored. First, on the left, instead of three layers, only two 1.5 mm layers were considered. In the right side, bulk or one increment technique was used. In this case, the effect of the variation of Young's modulus with depth is expected to be more important.

In order to examine the influence of the variation in stiffness on the final results, two models were developed with constant resin modulus of elasticity. The results are shown in Fig. 10, both for the complete restoration and for dentine, and show a reduction in stress levels. The real, variable distribution of Young's modulus through depth leads to an increase in stresses in the restoration. This effect is more pronounced for the one increment technique, as expected, as the stiffness variation is larger, and are in agreement with the work of Chiang et al., 2010.

When the influence of the cavity size and incremental restoration technique were analyzed in Class I restorations, it was verified that the adhesive was damaged in several locations, and cracks were occurring in the interface.

He et al. (2007) observed that the size of the restoration and the restoration technique affected its overall behavior. Incremental filling of the cavity reduced the stress levels in large cavities, but did not affect the resulting tractions for small restorations. The authors suggested that incremental technique be used in large restorations with a high C factor.

Sun et al. (2009) noted the occurrence of contraction at the top and base of the restorations, fact also observed in the present finite element simulation. Gaps formation is directly connected to the C factor and volume of composite resin, eventually leading to micro-leakages. The authors concluded that neither C-factor nor sample volume affects polymerization shrinkage at a constant Degree Conversion. They observed in an analysis with a micro-CT that resin contraction occurred independently of the geometry. Using either μCt or infiltration with dyes, if was possible to verify the occurrence of infiltration and its dependence on the C factor and resin volume.

As for Young's modulus and DC values for composite resin, it was expected that a stiffness reduction along the axial direction would lead to a reduction in residual stress levels. This was verified by Oliveira et al. (2010), using resins with low modulus of elasticity. The resulting gaps, even though reduced after hygroscopic expansion, were permanent, being observed even 4 years after treatment (Krämer et al., 2009). The complex behavior of light activated resins and the several parameters involved in its use, as discussed, reinforce the need and importance of further study in the area and the need to consider different aspects in the definition of the clinical restoration procedure (Kakaboura et al., 2007).

5. Concluding remarks

The results described in the previous sections point to the following conclusions:

- The polymerization device, when comparing Elipar and laser-driven devices, used to cure the resin, did not affect significantly the degree of cure (DC) of the examined samples.
- As for the thickness of the sample, for both polymerization devices, the results proved a high correlation between depth and DC value.
- The stiffness of the composite resin was affected by the thickness of the sample. This effect was more pronounced for depths larger than 2 mm
- The numerical analysis showed that layered techniques lead to improved stress distribution and reduced residual stresses in cylindrical restorations.
- The variation in elastic modulus in layers with thickness smaller than 2 mm is not pronounced. As for 3 mm layers, the resulting stress distribution is significantly different when compared with the results for a homogeneous stiffness through restoration thickness.
- The deterioration of the modulus of elasticity in thick layers led to a reduction in stress concentration in the model. Other relevant information, such as reduction in strength, change in contraction and quality of adhesion of the interface should be also investigated for a more complete picture of this case.
- Current recommendations for restricting layer thickness to 2 mm are in accordance with the obtained results.

6. Future directions

The reported results show that a refinement in finite element analysis can deepen the knowledge in the mechanical behavior of resin restorations, providing a tool to improve clinical success. Future work directions should include, among other aspects:

- examine the effect of hygroscopic expansion on the residual stress distribution;
- include inclined layers as an alternative to horizontal layers in the models;
- simulate drop-shaped cavities and restorations;
- study the consequences of the residual stresses and cracks in the performance of the restoration.

7. Acknowledgments

The authors kindly acknowledge the support of the Brazilian funding agencies FAPEMIG and CNPq in the development of this work.

8. References

Ansys Release 10.0.

Ausiello, P.; Apicella, A. & Davidson, C.L. (2002). Effect of adhesive layer properties on stress distribution in composite restorations - a 3D finite element analysis. *Dental Materials,* Vol.18, No.4, pp. 295-303, ISSN 0109-5641

Bouschlicher, M.R. & Rueggeberg, F.A. (2000). Effect of ramped light intensity on polymerization force and conversion in a photoactivated composite. *Journal of Esthetic Dentistry*, Vol.12, No.6, pp. 328-339, ISSN 1040-1466

Bowen R.L.; Nemoto, K. & Rapson, J.E. (1983). Adhesive bonding of various materials to hard tooth tissues: forces developing in composite materials during hardening. *Journal of the American Dental Association*, Vol.106, No.4, pp.475–477, ISSN 0002-8177

Braem, M.; Lambrechts, P.; Vanherle, G. & Davidson, C.L. (1987). Stiffness increase during the setting of dental composite resins. *Journal of Dental Research*, Vol.66, No.12, pp. 1713–1716, ISSN 0022-0345

Braga, R.R.; Ballestera, R.Y. & Ferracane, J.L. (2005). Factors involved in the development of polymerization shrinkage stress in resin-composites: A systematic Review. *Dental Materials,* Vol. 21, pp. 962–970, ISSN 0109-5641

Carvalho Filho, F. (2005). Modelagem via método dos elementos finitos da contração de resinas odontológicas fotopolimerizáveis, M. Sc. thesis, Structural Engineering, Engineering School, Federal University of Minas Gerais, UFMG (in Portuguese)

Ceballos, L.; Fuentes, M.V.; Tafalla, H.; Martínez, A.; Flores, J. & Rodríguez, J. (2009). Curing effectiveness of resin composites at different exposure times using LED and halogen units. *Journal of Clinical and Experimental Dentistry*, Vol.1, No.1, pp. 8-13, ISSN 1989-5488

Chiang, Y.C.; Rösch, P.; Dabanoglu, A.; Linc, C.P.; Hickel, R. & Kunzelmann, K.H. (2010). Polymerization composite shrinkage evaluation with 3D deformation analysis from μCT images. *Dental Materials*, Vol.26, No.3, pp. 223–231, ISSN 0109-5641

Cho, E.; Sadr, A.; Inai, N. & Tagami, J. (2011). Evaluation of resin composite polymerization by three dimensional micro-CT imaging and nanoindentation. *Dental Materials*, Vol.27, No.11, pp. 1070-1078, ISSN 0109-5641

Chung, K.H. & Greener, E.H. (1990). Correlation between degree of conversion filler concentration and mechanical properties of posterior composite resins. *Journal of Oral Rehabilitation*, Vol.17, No.5, pp. 487–494, ISSN 0305-182X

Dewaele, M.; Asmussen, E.; Peutzfeldt, A.; Munksgaard, E.C.; Benetti, A.R.; Finné, G.; Leloup, G. & Devaux, J. (2009). Influence of curing protocol on selected properties

of light-curing polymers: degree of conversion, volume contraction, elastic modulus, and glass transition temperature. *Dental Materials*, Vol.25, No.12, pp. 1576-1584, ISSN 0109-5641

Dietschi, D.; Monasevic, M.; Krejci, I. & Davidson, C. (2002). Marginal and internal adaptation of class II restorations after immediate or delayed composite placement. *Journal of Dentistry*, Vol.30, Nos.5-6, pp. 259–269, ISSN 0300-5712

Feilzer, A.J.; De Gee, A.J. & Davidson C.L. (1993). Setting stresses in composites for two different curing modes. *Dental Materials*, Vol.9, No.1, pp. 2–5, ISSN 0109-5641

Felix, C.A.; Price, R.B.T. & Andreou, P. (2006). Effect of reduced exposure times on the microhardness of 10 composites cured by high power LED and QTH curing lights. *Journal of the Canadian Dental Association*, Vol.72, No.2, pp. 147a–147g, ISSN 0008-3372

Ferracane, J.L. (2005). Developing a more complete understanding of stresses produced in dental composites during polymerization. *Dental Materials*, Vol.21, No.1, pp. 36–42, ISSN 0109-5641

Halvorson, R.H.; Erickson, R.L. & Davidson, C. L. (2002). Energy dependent polymerization of resin-based composite. *Dental Materials*, Vol.18, No.6, pp. 463–469, ISSN 0109-5641

He, Z.; Shimada, Y. & Tagami, J. (2007). The effects of cavity size and incremental technique on micro-tensile bond strength of resin composite in Class I cavities. *Dental Materials*, Vol.23, No.5, pp. 533–538, ISSN 0109-5641

Jandt, K.D.; Mills, R.W.; Blackwell, G.B. & Ashworth, S.H. (2000). Depth of cure and compressive strength of dental composites cured with blue light emitting diodes (LEDs). *Dental Materials*, Vol.16, No.1, pp. 41–47, ISSN 0109-5641

Jong, L.C.G.; Opdam, N.J.M.; Bronkhorst, E. M.; Roeters, J.J.M.; Wolke, J.G.C. & Geitenbeek, B. (2007). The effectiveness of different polymerization protocols for class II composite resin restorations. *Journal of Dentistry*, Vol.35, No.6, pp. 513-520, ISSN 0300-5712

Kakaboura, A.; Rahiotis, C.; Watts, D.; Silikas, N. & Eliades, G. (2007). 3D-marginal adaptation versus setting shrinkage in light-cured microhybrid resin composites. *Dental Materials*, Vol.23, No.3, pp. 272–278, ISSN 0109-5641

Kawaguchi, M.; Fukushima, T. & Horibe, T. (1989). Effect of monomer structure on the mechanical properties of light cured composite resins. *Dental Materials Journal*, Vol.8, No.1, pp. 40–45, ISSN 0287-4547

Krämer, N.; Reinelt, C.; Richter, G.; Petschelt, A. & Frankenberger, R. (2009). Nanohybrid vs. fine hybrid composite in Class II cavities: Clinical results and margin analysis after four years. *Dental Materials*, Vol.25, No.6, pp. 750–759, ISSN 0109-5641

Lim, B.-S.; Ferracane, J.L.; Sakaguchi, R.L. & Condon, J.R. (2002). Reduction of polymerization contraction stress for dental composites by two-step light-activation. *Dental Materials*, Vol.18, No.6, pp. 436–444, ISSN 0109-5641

Oliveira, L.C.A.; Duarte Jr., S.; Araujo, C.A. & Abrahão, A. (2010). Effect of low-elastic modulus liner and base as stress-absorbing layer in composite resin restorations. *Dental Materials*, Vol.26, No.3, pp. e159–e169, ISSN 0109-5641

Petrovic, L.M.; Drobac, M.R.; Stojanac, I.L. & Atanackovic, T.M. (2010). A method of improving marginal adaptation by elimination of singular stress point in composite

restorations during resin photo-polymerization. *Dental Materials*; Vol.26, No.5, pp. 449–455, ISSN 0109-5641

Peutzfeld, A. (1997). Resin composites in dentistry: The monomer systems. *European Journal of Oral Sciences*, Vol.105, No.2, pp. 97–116, ISSN 1600-0722

Peutzfeldt, A.; Sahafi, A. & Asmussen, E. (2000). Characterization of resin composites polymerized with plasma arc curing units. *Dental Materials*, Vol.16, No.5, pp. 330–336, ISSN 0109-5641

Rüttermann, S.; Krüger, S.; Raab, W. & Janda, R. (2007). Polymerization shrinkage and hygroscopic expansion of contemporary posterior resin-based filling materials—A comparative study. *Journal of Dentistry*, Vol. 35, No.10, pp. 806-813, ISSN 0300-5712

Sakaguchi, R. L.; Sasik, C. T.; Bunczak, M.A. & Douglas, W.H. (1991). Strain gauge method for measuring polymerization contraction of resin composite restoratives. *Journal of Dentistry*, Vol.19, No.5, pp. 312–316, ISSN 0300-5712

Silikas, N.; Eliades, G. & Watts, D.C. (2000). Light intensity effects on resin-composite degree of conversion and shrinkage strain. *Dental Materials*, Vol.16, No.4, pp. 292–296, ISSN 0109-5641

Sun, J.; Eidelman, N. & Gibson, S.L. (2009). 3D mapping of polymerization shrinkage using X-ray micro-computed tomography to predict microleakage. *Dental Materials*, Vol.25, No.3, pp. 314–320, ISSN 0109-5641

Yap, A.U.; Soh M.S. & Siow, K. S (2002). Effectiveness of composite cure with pulse activation and soft-start polymerization. *Operative Dentistry*, Vol.27, No.1, pp. 44–49, ISSN 0361-7734

Yoshikawa, T.; Burrow, M.F. & Tagami, J. (2001). A light curing method for improving marginal sealing and cavity wall adaptation of resin composite restorations. *Dental Materials*, Vol.17, No,4, pp. 359-366, ISSN 0109-5641

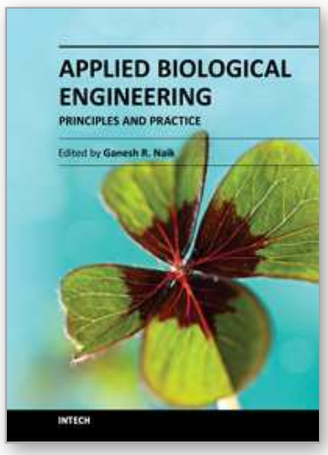

Applied Biological Engineering - Principles and Practice
Edited by Dr. Ganesh R. Naik

ISBN 978-953-51-0412-4
Hard cover, 662 pages
Publisher InTech
Published online 23, March, 2012
Published in print edition March, 2012

Biological engineering is a field of engineering in which the emphasis is on life and life-sustaining systems. Biological engineering is an emerging discipline that encompasses engineering theory and practice connected to and derived from the science of biology. The most important trend in biological engineering is the dynamic range of scales at which biotechnology is now able to integrate with biological processes. An explosion in micro/nanoscale technology is allowing the manufacture of nanoparticles for drug delivery into cells, miniaturized implantable microsensors for medical diagnostics, and micro-engineered robots for on-board tissue repairs. This book aims to provide an updated overview of the recent developments in biological engineering from diverse aspects and various applications in clinical and experimental research.

INTECH
open science | open minds

InTech Europe
University Campus STeP Ri
Slavka Krautzeka 83/A
51000 Rijeka, Croatia
Phone: +385 (51) 770 447
Fax: +385 (51) 686 166
www.intechopen.com

InTech China
Unit 405, Office Block, Hotel Equatorial Shanghai
No.65, Yan An Road (West), Shanghai, 200040, China
中国上海市延安西路65号上海国际贵都大饭店办公楼405单元
Phone: +86-21-62489820
Fax: +86-21-62489821

IntechOpen